Available online at www.sciencedirect.com
SCIENCE DIRECT®
Surface Science 566–568 (2004) 337–342
SURFACE SCIENCE
www.elsevier.com/locate/susc

Effect of CO on the morphology of Pt nanoparticles supported on $TiO_2(1\,1\,0)$-$(1\times n)$

A. Berkó *, J. Szökő, F. Solymosi

Institute of Solid State and Radiochemistry, Reaction Kinetics Research Group of the Hungarian Academy of Sciences, University of Szeged, P.O. Box 168, 6701 Szeged, Hungary

Available online 7 June 2004

Abstract

The effect of CO on the morphology of Pt nanoparticles of different sizes (1–4 nm) supported on $TiO_2(1\,1\,0)$-$(1\times n)$ surface was investigated by scanning tunnelling microscopy (STM). The CO pressure was varied in the range of 10^{-3}–10^{1} mbar. It was found that CO adsorption induces a significant increase in the initial size of the Pt nanoparticles of 1–2 nm even at room temperature. The agglomeration, however, is characteristically preceded by disruption of the smaller Pt nanoclusters at lower CO pressures. This finding was explained by CO-assisted Ostwald ripening, in which the mass transport proceeds via surface carbonyl intermediates.

Keywords: Carbon monoxide; Surface structure, morphology, roughness, and topography; Platinum; Clusters; Growth; Titanium oxide; Scanning tuneling microscopy

1. Introduction

The change of the morphology of supported metal nanoparticles in ambient gas atmospheres is of great interest, because this process is decisively important in the heterogeneous catalysis [1–6]. There are some fundamental topics related to this field: (i) preparation of the supported metal particles on oxide single crystals; (ii) characterization of these samples by low-pressure adsorption of different gases; (iii) thermally induced processes (adsorption, reaction, desorption) on nanoparticle-arrangements; (iv) high pressure experiments on two-dimensional model catalysts. While in the first two topics a great leap forward was attained during the last few years, the foregoing results are far from complete in the latter two cases.

It is widely accepted that morphological changes of supported metal nanoclusters (crystallites) can be induced by gases adsorbed strongly on the particles at high pressures ($p > 1$ mbar), the occurrence of which depends on the size of the metal nanoparticles [6–18]. A special case of the particle-restructuring on the effect of gas adsorption is the so called oxidative disruption and reductive agglomeration of the supported noble metal nanoparticles observed in CO ambient [7,8,19–26]. In these studies several structure sensitive methods were applied, like EXAFS, FTIR, STM. The main part of these efforts concentrated on the spectroscopic detection of the carbonyl

* Corresponding author. Tel.: +36-62-544-803; fax: +36-62-420-678.
E-mail address: aberko@chem.u-szeged.hu (A. Berkó).

0039-6028/$ - see front matter © 2004 Elsevier B.V. All rights reserved.
doi:10.1016/j.susc.2004.05.065

species involved in the structural changes [16,17, 19–27]. The other part of the works relates to the change of the morphology of metal particles [7–15,18]. It is clear from these studies that the fine details of the disruption and agglomeration (especially the kinetics of the process) depend sensitively on the chemical nature of the support and the metal supported on it. For example, while formation of gem-dicarbonyl species (due to oxidative disruption) readily appeared in the case of Rh and Ir supported on oxides [19–25], it was difficult to detect on supported Pt ([26] and references therein).

In this paper the effects of CO treatments are investigated on the morphology of Pt nanoparticles supported on $TiO_2(1\,1\,0)$-$(1\times n)$ surface by scanning tunnelling microscopy.

2. Experimental

The experiments were carried out in an UHV chamber equipped with a room temperature scanning tunnelling microscope, a cylindrical mirror analyzer applied for Auger-electron spectroscopy (AES) and a quadrupole mass spectrometer for gas analysis. More experimental details can be found in [7].

$TiO_2(1\,1\,0)$ single crystal was clipped on a Ta-plate mounted to a transferable sample holder and heated by radiation of a W-filament. The temperature of the probe was measured by a chromel–alumel thermocouple sticked by oxide adhesive (ceramobond 571, Aremco Products). A typical cleaning procedure consisted of 5 min Ar^+ bombardment (1 keV) and 10 min annealing at 1100 K. From time to time the surface was re-oxidized in 10^{-6} mbar oxygen at 800 K.

The cleanness of the sample and the metal overlayer was checked by AES. The Pt-coverage is expressed in monolayer equivalent (ML), which corresponds to 1.6×10^{15} atom/cm^2. The actual coverage was calculated by determination of the total volume of the well separated 3D metal nanoparticles formed upon annealing at 1100 K and by taking into account the atom density of the Pt [27,28].

For STM imaging chemically edged W-tips were applied and sharpened "in situ" above the TiO_2 surface by applying 5–10 V pulses. Typical tunnelling parameters of +1.5 V and 0.2 nA were used for imaging.

Pt was deposited by glowing of a high purity (99.95%) Pt filament. Particularly, in the case of the Pt/TiO_2 catalysts, which is one of the best known SMSI (decoration) system, the high temperature annealing in vacuum (reductive circumstances) may cause decoration of the Pt particles by a reduced phase of the support [33,34]. For an SMSI catalyst, the CO-induced morphology change may radically be restrained because the adsorption of CO is totally hindered. Accordingly, in this work we use only room temperature deposition followed by gentle annealing (400 K) of the model catalysts.

3. Results and discussion

3.1. Preparation and characterization of Pt nanoparticle-arrays on $TiO_2(1\,1\,0)$-$(1\times n)$ support

$TiO_2(1\,1\,0)$-$(1\times n)$ support showed characteristic added rows running in the direction of [0 0 1] (Fig. 1A). The one dimensional rows randomly separated by $n*0.65$ nm ($2<n<5$) can be attributed to the epitaxially grown Ti_2O_3 rows of 0.12 nm of height and 30–40 nm of length. The interrow areas can be identified as (1×1) terraces. The characteristic morphology of the $TiO_2(1\,1\,0)$ surface annealed at high temperature (1100 K) was discussed in details in several papers [29–32].

In Fig. 1B and C the $Pt/TiO_2(1\,1\,0)$-$(1\times n)$ surfaces are imaged after deposition of 0.08 and 1.50 ML Pt at 300 K followed by annealing at 400 K, respectively. The fine analysis of the images obtained after deposition of 0.08 ML Pt has shown that the size-distribution of the Pt nanoparticles is rather wide: the small particles of 1–2 nm (10–100 Pt atoms) bond characteristically on the (1×1) terraces and the largest ones of 3–4 nm (300–3000 Pt atoms) are localized mainly at the end of the 1D rows (Fig. 1B). The higher deposition of Pt (1.5 ML) does not cause any radical increase of the particle size (the average diameter is 4–5 nm), although the surface is completely covered by nanoparticles of this size (Fig. 1C).

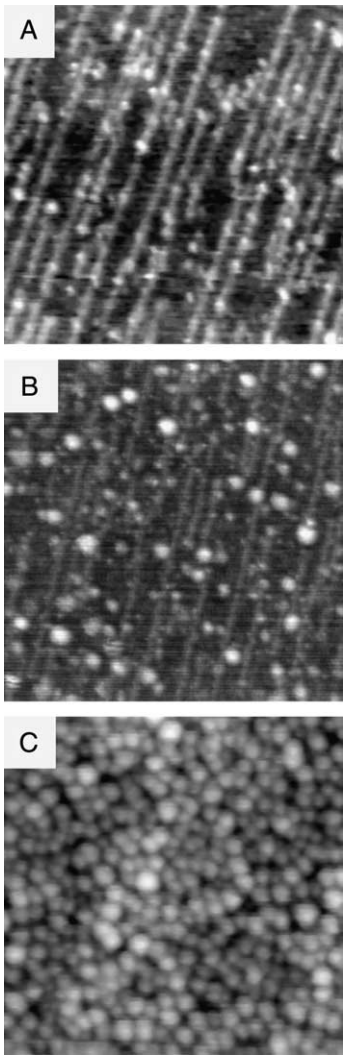

Fig. 1. Characteristic STM images (50 nm × 50 nm) recorded on (A) clean and Pt-deposited (B) 0.08 ML, (C) 1.50 ML $TiO_2(1\,1\,0)$-$(1\times n)$ surface. The evaporation of Pt was performed at 300 K followed by a gentle annealing at 400 K in UHV.

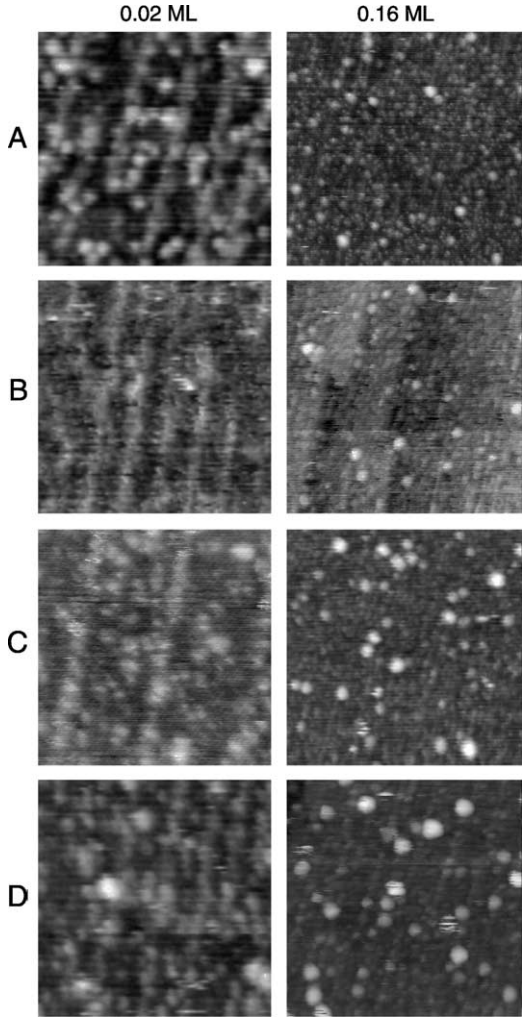

Fig. 2. Effects of CO-exposure at 300 K on $Pt/TiO_2(1\,1\,0)$-$(1\times n)$ surface for two different metal coverages: 0.02 ML, 0.16 ML. (A) Initial morphology of the model catalysts; after 10 min exposure of CO (B) 10^{-3} mbar, (C) 10^{-1} mbar, (D) 10 mbar. The size of the images: 20 nm × 20 nm (left), 50 nm × 50 nm (right).

3.2. Effects of CO on the morphology of the Pt nanoparticles

In the next experiments the effect of CO exposure is studied over Pt deposited on a $TiO_2(1\,1\,0)$-$(1\times n)$ surface at two coverages and annealed gently at 400 K.

Results obtained at 0.02 ML of Pt coverage are shown on the left side of Fig. 2A–D. The size of the images is 20 nm × 20 nm. The characteristic area imaged before the CO treatments exhibits Pt nanoparticles of 1–2 nm distributed more or less homogeneously (Fig. 2A). On the effect of CO exposure (10 min, 10^{-3} mbar) the particles of 1–2 nm totally disappeared, only very finely dispersed dots can be seen (Fig. 2B). This feature can be regarded as a sign for desintegration (disruption) of Pt nanoparticles. This tendency reverses

however, as the exposure of CO increases (10 min, 10^{-1} mbar): the 1–2 nm particles reappear with nearly the same concentration (Fig. 2C). At higher CO exposure (10 min, 10 mbar), the agglomeration of the particles proceeds and a few larger particles (2–3 nm) are readily observed. It is worth mentioning that the further annealing of this surface even at 1100 K in UHV results in only a slight change.

The same CO treatment was performed for the model catalyst containing 0.16 ML Pt (Fig. 2, right side). The size of these STM images was 50 nm × 50 nm. Before CO treatment, the size of the Pt-particles varied in the range of 1–3 nm (Fig. 2A). Exposing this surface to CO (10 min, 10^{-3} mbar) at 300 K, only very limited change of the morphology of the surface was observed: the concentration of the larger nanoparticles increased to some extent (Fig. 2B). A significant increase in the average particle size was experienced, however, on the effect of further CO exposure (10^{-1} mbar, 10 min): the concentration and the average size of the larger particles increased by a factor of two (Fig. 2C). Only a slight further increase of these parameters was experienced by exposing the sample to 10 mbar CO for 10 min.

The STM images presented in Fig. 3 shows a large scale (100 nm × 100 nm) changes of the Pt/TiO_2(1 1 0)-(1 × n) model catalyst in the presence of CO and after postannealing in vacuum at high temperature (1100 K). In this case, 0.16 ML Pt was deposited on the TiO_2 at 300 K (Fig. 3A). The STM pictures clearly show that neither the atomic steps and nor the 1D rows of the support terraces are decorated preferentially. Pt nanoparticles of 1–3 nm cover rather uniformly the three terraces imaged. As presented above, CO exposure (10 mbar, 10 min, 300 K) results in a considerable increase in the particle diameter up to 5 nm (Fig. 3B). The same CO exposure at 500 K causes only a slight modification in the average morphology (Fig. 3C). It should be noted that the annealing in CO at above 600 K produces a more substantial change in the morphology (not shown here). This latter process is probably caused by the dissociation of CO and formation of C deposits, the study of which is out of the scope of this paper [35,36]. The annealing of the CO-exposed surface in vac-

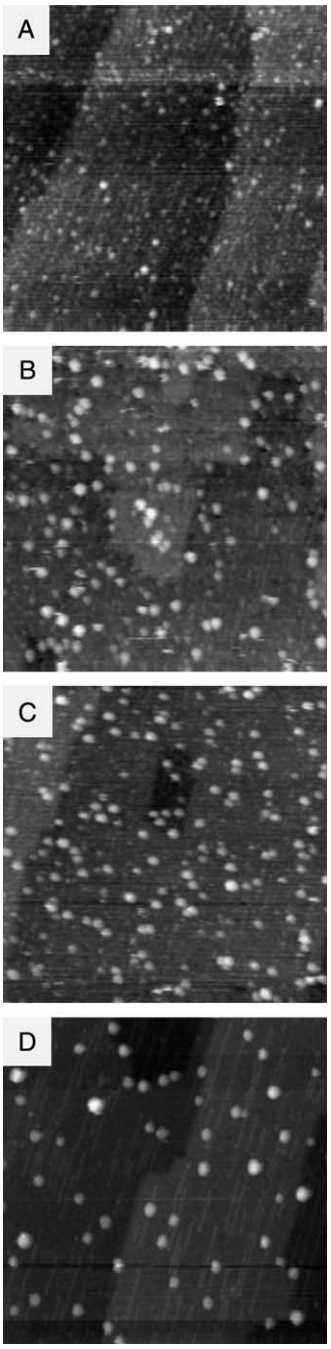

Fig. 3. Alteration of the distribution of Pt nanoparticles on the effect of the treatment in CO and UHV at different temperatures. (A) Initial morphology after deposition of Pt (0.16 ML) at 300 K followed by annealing at 400; (B) after exposure in 10 mbar CO for 10 min at (B) 300 K and (C) 500 K, (D) followed by annealing at 1100 K in UHV for 10 min.

uum at 1100 K led to some further decrease of the particle concentration and a slight increase of the average size (Fig. 3D).

3.3. Interpretation of CO-assisted change of the metal nanoparticles

The shape reforming of the supported nanoparticles involves numerous elementary steps determining the kinetics of the process and each step is governed by the local chemistry of the system. The previous papers dealing with the understanding of CO-induced disruption concentrated mainly on the appearance (and detection) of dicarbonyl species which were taken into account in explanation of the driving force of the morphological changes [19–26]. However, it is obvious that the surface diffusion of the different species participating in the particle reformation also plays an important role. Moreover, the effect of the pressure of the gas phase is also not negligible, because the impinging molecules modify continuously the local energy balance.

Two different types of particle-reformation can be distinguished: (i) the change of the particle shape (spreading, collapse, faceting); (ii) the change of the integrity (disruption and agglomeration) of the nanoparticles. The basic difference between these processes is that the first one involves atom diffusion on the particle (or at the particle-support interface), while the second one refers to the separation/condensation of the metal atoms from/to the particles and to their diffusion on the support. In both cases the adsorbed gas molecule weakens the bond of a metal atom to its neighbouring atoms, and facilitates the diffusion (mass transport) of the surface species.

The important conclusion drawn from the experimental results presented above is that CO pressure larger than 10^{-1} mbar causes a very rapid agglomeration of the supported Pt nanoparticles even at room temperature. It can clearly be seen from the STM images (Fig. 3) that the extent of the agglomeration in this process is just the same as that after annealing in UHV at 1100 K. From this fact it is evident that CO induces a large mass transport among the metal nanoparticles. Substantially two types of mechanism can be assumed: (i) the gas-assisted Ostwald ripening, where the less stable (smaller) particles release atoms on the effect of adsorption and the released atoms condense to the more stable (larger) ones; (ii) the collective diffusion of the smaller nanoparticles covered by adsorbed molecules and the subsequent collapse of the colliding particles. This latter mechanism was clearly observed only for tiny ($d < 1$ nm) metal nanoparticles (without application of gas-ambient) [37]. Nevertheless, the fact that particle-agglomerates were characteristically not observed (at least for the particles larger than 1 nm) in our experiments, strongly suggests that the gas-assisted Ostwald ripening is the main mechanism in the CO-induced particle-reformation.

In our earlier studies it was found that in the case of Rh and Ir nanoparticles supported on a TiO_2(1 1 0) surface both the desintegration and the agglomeration of the nanocrystallites proceed depending on the size of the particles and on the pressure of CO [7,8]. This behaviour is quite similar in many respects to the case of Pt, however the agglomeration of this metal is more pronounced at higher CO pressures. This feature may be explained by the lower stability of surface Pt-carbonyls.

4. Conclusions

It was shown that the Pt nanoparticles (average diameter of 1–2 nm) formed by deposition of the metal at 300 K (and postannealed at 400 K) agglomerate readily into larger particles (3–4 nm) on the effect of CO exposure at a pressure of 10 mbar and temperature of 300 K. This process can be explained by gas-assisted Ostwald ripening which involves also the desintegration (disruption) of the smaller Pt nanoparticles consisting of few atoms.

Acknowledgements

The authors express their grateful thanks for the valuable discussions to Dr. János Raskó. This work was supported by the Hungarian Scientific

Research Fund (OTKA) through TS40877, T32040 and T43057 projects.

References

[1] M. Bäumer, H.-J. Freund, Prog. Surf. Sci. 61 (1999) 127.
[2] C.T. Campbell, Surf. Sci. Rep. 27 (1997) 1.
[3] C.R. Henry, Surf. Sci. Rep. 31 (1998) 231.
[4] U. Diebold, Surf. Sci. Rep. 48 (2003) 53.
[5] D.W. Goodman, Surf. Rev. Lett. 2 (1995) 9.
[6] P.L.J. Gunter, J.W.H. Niemantsverdriet, F.H. Ribeiro, G.A. Somorjai, Catal. Rev. Sci. Eng. 39 (1997) 77.
[7] A. Berkó, F. Solymosi, J. Catal. 183 (1999) 91.
[8] A. Berkó, F. Solymosi, Surf. Sci. 411 (1998) L900.
[9] P.L. Hansen, J.B. Wagner, S. Helveg, J.R. Rostrup-Nielsen, B.S. Clausen, H. Topsøe, Science 295 (2002) 2053.
[10] M. Kalff, G. Comsa, T. Michely, Phys. Rev. Lett. 81 (6) (1998) 1255.
[11] T. Hill, M. Mozaffari-Afshar, J. Schmidt, T. Risse, S. Stempel, M. Heemeier, H.-J. Freund, Chem. Phys. Lett. 292 (1998) 524.
[12] C. Voss, N. Kruse, Surf. Sci. 409 (1998) 252.
[13] H. Graoui, S. Giorgio, C.R. Henry, Surf. Sci. 417 (1998) 350.
[14] B.J. McIntyre, M. Salmeron, G.A. Somorjai, J. Vac. Sci. Technol. A 11 (4) (1993) 1964.
[15] G. Rupprechter, G. Seeber, H. Goller, K. Hayek, J. Catal. 186 (1999) 201.
[16] A. Sandell, J. Libuda, M. Bäumer, H.-J. Freund, Surf. Sci. 346 (1996) 108.
[17] J. Libuda, A. Sandell, M. Bäumer, H.-J. Freund, Chem. Phys. Lett. 240 (1995) 429.
[18] A. Kolmakov, D.W. Goodman, Surf. Sci. 490 (2001) L597.
[19] F. Solymosi, M. Pásztor, J. Phys. Chem. 89 (1985) 4789.
[20] P. Basu, D. Panayotov, J.T. Yates jr., J. Am. Chem. Soc. 110 (1988) 2074.
[21] D.A. Buchanan, M.E. Hernandez, F. Solymosi, J.M. White, J. Catal. 125 (1990) 456.
[22] H.F.J. van't Bilk, J.B.A.D. van Zon, T. Huizinga, J.C. Vis, D.C. Koningsberger, R. Prins, J. Am. Chem. Soc. 107 (1985) 3139.
[23] D.A. Bulushev, G.F. Froment, J. Mol. Catal. A 139 (1999) 63.
[24] J. Evans, B.E. Hayden, M.A. Newton, Surf. Sci. 462 (2000) 169.
[25] J. Evans, B.E. Hayden, F. Mosselmans, A. Murray, J. Am. Chem. Soc. 114 (1992) 6912.
[26] J. Raskó, J. Catal. 217 (2003) 478.
[27] A. Berkó, F. Solymosi, Surf. Sci. 400 (1998) 281.
[28] A. Berkó, G. Klivényi, F. Solymosi, J. Catal. 182 (1999) 511.
[29] S. Takakusagi, K. Fukui, F. Nariyuki, Y. Iwasawa, Surf. Sci. 523 (2003) L41.
[30] R.A. Bennett, P. Stone, N.J. Price, M. Bowker, Phys. Rev. Lett. 82 (19) (1999) 3831.
[31] S. Fischer, A.W. Munz, K.D. Schierbaum, W. Göpel, Surf. Sci. 337 (1995) 17.
[32] M. Li, W. Hebenstreit, U. Diebold, Phys. Rev. B 61 (7) (2000) 4926.
[33] A. Berkó, I. Ulrych, K.C. Prince, J. Phys. Chem. B 102 (1998) 3379.
[34] O. Dulub, W. Hebenstreit, U. Diebold, Phys. Rev. Lett. 84 (16) (2000) 3646.
[35] K.Y. Kung, P. Chen, F. Wei, Y.R. Shen, G.A. Somorjai, Surf. Sci. 463 (2000) L627.
[36] S. Gan, Y. Liang, D.R. Baer, M.R. Sievers, G.S. Herman, C.H.F. Peden, J. Phys. Chem. B 105 (2001) 2412.
[37] M.J.J. Jak, C. Konstapel, A. van Kreuningen, J. Verhoeven, J.W.M. Frenken, Surf. Sci. 457 (2000) 295.